Cite this: DOI: 10.1039/xxxxxxxxxx

Molecular synthons for accurate structural determinations: the equilibrium geometry of 1-chloro-1-fluoroethene

Alberto Gambi,*[a] Andrea Pietropolli Charmet,[b] Paolo Stoppa,[b] Nicola Tasinato,[c] Giorgia Ceselin,[c] and Vincenzo Barone [c]

Received Date
Accepted Date

DOI: 10.1039/xxxxxxxxxx

www.rsc.org/journalname

Equilibrium structure for the 1-chloro-1-fluoroethene is reported. The structure has been obtained by a least-squares fit procedure using the available experimental ground-state rotational constants of eight isotopologues. Vibrational effects have been removed from the rotational constants using the vibration-rotation interaction constants derived from computed quadratic and cubic force fields obtained with the required quantum chemical calculations carried out by using both coupled cluster and density functional theory. The semi-experimental geometry obtained in this way has been also compared with the corresponding theoretical predictions obtained at CCSD(T) level after extrapolation to the complete basis set limit and inclusion of core-valence corrections. These results allow to complete the molecular geometries of the isomers of chlorofluoroethene in addition the *cis* and *trans* forms of 1-chloro-2-fluoroethene already published.

1 Introduction

The concerns due to the role of halogenated molecules as organic trace pollutants[1–4] have motivated many of the theoretical and experimental studies on these compounds that have appeared in the literature. High-resolution spectroscopic techniques are able to provide detection (and quantification) of these species in the atmosphere,[5] but they require accurate spectroscopic data (obtained by investigations focused on line positions,[6–10] intensities,[11,12] and broadening coefficients[13]) which, in turn, must be obtained from the analysis of highly congested spectra, very often complicated by the effects of anharmonic and Coriolis interactions.[14–17] Anyway, recent improvements in both the experimental techniques and the theoretical methods are nowadays able to efficiently support and guide the spectroscopic investigations. At present, high-level *ab initio* calculations[18–20] can provide reliable anharmonic force fields required to take into account all the resonances and also yield the predictions in band positions and intensities, and therefore in recent years they have been successfully applied to the vibrational analysis of many halocarbons.[21–29]

For a comprehensive understanding of the physical chemical properties of a molecule, the geometrical structure is mandatory; furthermore it provides fundamental reference data whose determination is the first step toward the challenge of accurate structural determinations for systems of increasing size.[30,31] Several methods are available for experimental structure determination, however when accurate geometries are needed, rotational spectroscopy is usually the method of choice.[32]

However, for polyatomic molecules, the determination of equilibrium structures is not a simple task due to the large number of structural parameters that must be determined by the analysis of the rotational spectra of several isotopically substituted species. Another problem is the consideration of the vibrational effects.

Quantum chemical calculations are of great help also from this perspective because not only they can determine the theoretical equilibrium structure but they are also able to provide the spectroscopic parameters necessary to evaluate the vibrational corrections. Accurate quantum chemical geometries can usually be obtained by using highly correlated wavefunction methods possibly coupled to composite schemes accounting for missing effects such as core-valence correlations and complete basis set extrapolations.[31,33–35] Hence, from both experimental and theoretical points of view, obtaining accurate equilibrium geometries becomes prohibitive but for very small molecules. In this respect, a notable improvement is represented by the so-called semi-experimental approach, first introduced by Pulay and coworkers.[36] This integrated experimental-theoretical strategy relies on inverting experimental spectroscopic results to equilibrium structures by employing quantum chemical calculations in order to account for the vibrational (and potentially electronic) contri-

---

[a] *Address, Università degli Studi di Udine, Dipartimento Politecnico di Ingegneria e Architettura, Via Cotonificio 108, I-33100 Udine, Italy. Fax: +39 0432 558803; Tel: +39 0432 558856; E-mail: alberto.gambi@uniud.it*

[b] *Address, Università Ca' Foscari Venezia, Dipartimento di Scienze Molecolari e Nanosistemi, Via Torino 155, I-30172 Mestre (VE), Italy.*

[c] *Address, Scuola Normale Superiore, Piazza dei Cavalieri 7, I-56126 Pisa, Italy.*

butions. Over the last few years the semi-experimental approach has been exploited for several small to medium size molecular systems, leading to the compilation of a database storing accurate molecular structures for about sixty molecules containing up to fifteen atoms.[37–39] While such a database provides an invaluable benchmark for the development of new computational methods rooted into quantum or classical mechanics,[40–42] one of the challenges for accurate quantum chemical investigations of equilibrium structures is the extension toward systems of increasing size. Here again the availability of reference equilibrium geometries represents the cornerstone to accomplish this target. In the attempt to increase the size of systems amenable to quantum chemical equilibrium structure determination, two approaches, namely the templating molecule approach (TMA) and the linear regression approach (LRA), have been proposed to improve the geometrical parameters optimized by methods rooted into density functional theory.[37,38]

The microwave spectrum of 1-chloro-1-fluoroethene was first measured by Stone and Flygare[43] and later in the millimeter wave region by Alonso *et al.*[44] by means of two-dimensional Fourier transform spectroscopy. Recently, Leung *et al.*[45] reported the microwave spectra of eight isotopic modifications of $ClFC{=}CH_2$ with the respective rotational constants together other spectroscopic parameters.

Concerning the geometry, besides the determination of a Kraitchman substitution structure, an empirical structure derived from a fit of the ground state moments of inertia of the eight isotopologues[45] was also obtained.

The aim of this work is to determine the accurate equilibrium structure of 1-chloro-1-fluoroethene. Two different techniques have been employed: *ab initio* geometry optimization at a high level of theory through the application of two basis set extrapolation schemes, and a semi-experimental structure calculation from the rotational constants of eight isotopologues[45] corrected with vibrational corrections computed theoretically. These corrections have been obtained from both the *ab initio* and DFT cubic force field for the normal modes of the different isotopologues of $ClFC{=}CH_2$.

In Section 2, the *ab initio* anharmonic force field, the semi-experimental structure and the complete basis set equilibrium geometry are given. Section 3 presents the results obtained and discusses the chemically relevant features of the structures of 1-chloro-1-fluoroethene. In addition, DFT optimized geometries are compared with the semi-experimental structure and it is shown how the LRA can be used to obtain an improved description of DFT geometrical parameters. Concluding, the different structures of the three chloro-fluoroethene isomers, namely $ClFC{=}CH_2$, *trans*-$ClHC{=}CHF$ and *cis*-$ClHC{=}CHF$ will be presented and commented.

2 Computational details and methods

2.1 Harmonic and anharmonic force fields

For each isotopologue, the quadratic and cubic force constants in term of the mass-independent internal coordinates, have been transformed into the normal coordinates representation.

The harmonic (quadratic) and the complete cubic anharmonic force fields have been evaluated at the coupled cluster level of theory with single and double excitations augmented by a perturbational estimate of the effects of connected triple excitations,[46] CCSD(T). These calculations have been performed with a local version of the CFOUR program package.[47]

Several different correlation consistent Dunning basis sets have been employed in order to get the best frequency evaluation, as reported in the previous work.[48] To be more precise, to account for the electronegative character of the F and Cl atoms, and for an adequate treatment of core and core-valence correlation effects on molecular geometry, the correlation-consistent polarized core-valence triple zeta basis (cc-pCVTZ) has been employed for H, C, and Cl atoms while for the F atom the aug-cc-pCVTZ basis set has been used in order to improve the overestimated C−F stretching frequency.[49–52] For conciseness, these basis sets will be referred as AFCVTZ in the continuation of the text. Spherical harmonics have been used throughout and all the electrons have been correlated excluding the $1s$ electrons of the chlorine atom.[52]

At the computed equilibrium geometry, the harmonic force constants have been obtained, in Cartesian coordinates, using analytic second derivatives of the energy.[53] The corresponding cubic force field has been determined in a normal-coordinates representation with the use of a finite difference procedure[54] involving displacements along reduced normal coordinates[55] (step size $\Delta Q = 0.05\,\mathrm{u}^{1/2} a_0$) and the calculation of analytic second derivatives at these displaced geometries.

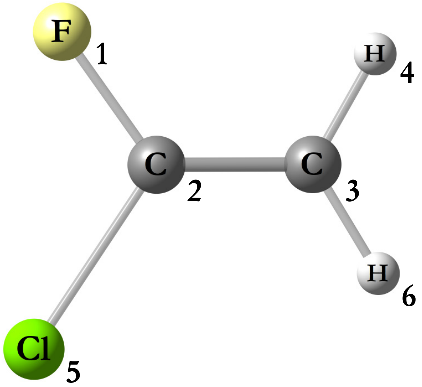

Fig. 1 Molecular structure of $ClFC{=}CH_2$ and numbering of its atoms.

The quadratic and cubic force constants have been initially obtained for the main isotopologue ($H_2C{=}C^{35}ClF$) and then transformed to the mass-independent internal coordinates representation. The molecule of 1-chloro-1-fluoroethene belongs to the C_s symmetry point group. A chemically intuitive non-redundant set of internal coordinates can be chosen to have $9A'$ internal coordinates, which lie in the molecular symmetry plane and correspond to the structural parameters, and $3A''$ out of plane internal coordinates that describe the vibrational modes outside this plane. These internal coordinates are defined in Table 1 where the labeling of the atoms is shown in Fig. 1. In the same Table the molecular geometry calculated at the CCSD(T)/AFCVTZ level of theory is also reported.

Table 1 Definition of the internal coordinates used to get the mass-independent force field. In the last column are shown the structural parameter – bond lengths in Å and bond angles in degrees – computed at the CCSD(T)/AFCVTZ level of theory

Symmetry Species	Internal Coordinates	Description	Geometry
A'	R_1	C_2-F_1	1.3344
	R_2	$C_2=C_3$	1.3252
	R_3	C_3-H_4	1.0790
	R_4	C_2-Cl_5	1.7140
	R_5	C_3-H_6	1.0767
	R_6	$\angle C_3=C_2-F_1$	122.27
	R_7	$\angle C_3=C_2-Cl_5$	125.87
	R_8	$\angle C_2=C_3-H_6$	120.12
	R_9	$\angle C_2=C_3-H_4$	119.37
A''	R_{10}	$F_1-(Cl_5-C_2=C_3)$	
	R_{11}	$H_4-(H_6-C_3=C_2)$	
	R_{12}	$Cl_5-C_2=C_3-H_6$	

Since the symmetry of the force constants should belong to the totally symmetry species A', the force field will be composed as follows: the quadratic force constants will be 51 detailed as $45A'A'$ and $6A''A''$, whereas the cubic force constants are 219 detailed as $165A'A'A'$ and $54A''A''A'$. Employing the internal coordinates defined in Table 1, the quadratic and cubic force fields reported, respectively, in Table 2 and Table 3, have been obtained.

Table 2 Quadratic force constants in internal coordinates, F_{ij}, at CCSD(T)/AFCVTZ level of theory: the units of the force constants are consistent with energy in aJ, bond lengths in Å and bond angles in rad

i	j	F_{ij}	i	j	F_{ij}	i	j	F_{ij}
1	1	6.490	6	3	−0.040	8	7	0.001
2	1	0.443	6	4	−0.517	8	8	0.902
2	2	9.615	6	5	0.047	9	1	−0.028
3	1	−0.007	6	6	2.086	9	2	0.226
3	2	0.034	7	1	−0.546	9	3	0.037
3	3	5.756	7	2	0.292	9	4	0.064
4	1	0.567	7	3	0.041	9	5	−0.117
4	2	0.328	7	4	0.010	9	6	−0.039
4	3	−0.001	7	5	−0.033	9	7	0.069
4	4	4.123	7	6	1.098	9	8	0.416
5	1	−0.016	7	7	1.834	9	9	0.892
5	2	0.011	8	1	0.078	10	10	2.186
5	3	0.005	8	2	0.271	11	10	0.448
5	4	−0.008	8	3	−0.119	11	11	0.877
5	5	5.835	8	4	0.002	12	10	0.680
6	1	0.158	8	5	0.024	12	11	0.460
6	2	0.356	8	6	0.091	12	12	0.514

Subsequently, for each isotopologue for which experimental ground-state rotational constants are available,[45] the cubic force fields have been used to compute the spectroscopic parameters. Table 4 reports the spectroscopic parameters computed for six additional isotopologues of 1-chloro-1-fluoroethene, and to be more precise $H_2C{=}^{13}C^{35}ClF$, $H_2C{=}^{13}C^{37}ClF$, $H_2{}^{13}C{=}C^{35}ClF$, $H_2{}^{13}C{=}C^{37}ClF$, (E)$-HDC{=}C^{35}ClF$, and (Z)$-HDC{=}C^{37}ClF$, in addition to those reported for $H_2C{=}C^{35}ClF$ and $H_2C{=}C^{37}ClF$ in the previous work[48] on the vibrational spectra and absorption cross sections of this molecule.

Table 4 lists also the diagonal elements of the inertial chlorine and deuterium quadrupole tensor, χ_{ij}, obtained at the same level of theory. The elements of this tensor, evaluated from an applied field gradient q_{ij}, have been calculated with the formula

$$\chi_{ij}(\mathrm{MHz}) = 234.9647 \cdot Q(\mathrm{b}) \cdot q_{ij}(\mathrm{au}) \qquad i,j = a,b,c \tag{1}$$

where Q is the nuclear electric quadrupole moment of chlorine or deuterium nucleus in units of barn[56] and a, b, and c are the inertial axes. Due to the molecular planarity, the inertial nuclear quadrupole tensor has only the χ_{ab} off-diagonal element.

In addition the cubic force field required to compute the vibrational corrections to rotational constants, has been evaluated from density functional theory (DFT) calculations for all the required isotopologues. Both the B3LYP[57,58] functional in conjunction with the SNSD[59] basis set and the double hybrid B2PLYP[60] functional coupled to the cc-pVTZ[49,50] basis set have been employed. All DFT calculations have been performed by using the Gaussian16 quantum chemical package,[61] with the vibrational corrections to rotational constants obtained within the generalized vibrational perturbative engine.[62]

2.2 Semi-experimental equilibrium geometry

Subsequently, The vibration-rotation interaction constants α_r^i (where r denotes the vibrational normal mode and $i = a$, b, or c the inertial axis) have been computed using expressions from the vibrational second-order perturbation theory (VPT2), which has the advantage to have analytical formulas for obtaining the spectroscopic parameters.[63,64]

To VPT2, the equilibrium molecular rotational constants B_e^i is related to the vibrational ground state rotational constants B_0^i as

$$B_e^i = B_0^i + \frac{1}{2}\sum_r \alpha_r^i \qquad i = a,b,c \tag{2}$$

where the summation is over the $r = 3N-6$ vibrational modes, N being the number of nuclei.

The rotational constants B_e^i is inversely proportional to the principal moment of inertia I_i at the equilibrium geometry, and within the Born-Oppenheimer approximation, the equilibrium geometry is the same for all isotopologues.

The semi-experimental equilibrium structure r_e^{SE} has been obtained by a least-squares fit of the molecular structural parameters, corresponding to the planar internal coordinates of symmetry species A', listed in Table 1, to the given experimental rotational constants corrected for the vibrational contributions computed theoretically. Actually, the fit requires at least as many independent rotational constants as there are structural degrees of freedom: for 1-chloro-1-fluoroethene, 5 bond lengths and 4 bond angles are needed as listed in Table 1. However, using more rotational constants, when available, is preferred since in this way the consistency of the experimental data can be checked.

It should be also mentioned that being 1-chloro-1-fluoroethene a planar molecule, only two of the three rotational constants are independent and can be included in the fit, since the relation

$$1/C = 1/A + 1/B$$

Table 3 CCSD(T)/AFCVTZ level of theory cubic force constants in internal coordinates, F_{ijk}: the units of the force constants are consistent with energy in aJ, bond lengths in Å and bond angles in rad

i	j	k	F_{ijk}	i	j	k	F_{ijk}	i	j	k	F_{ijk}	i	j	k	F_{ijk}	i	j	k	F_{ijk}
1	1	1	−41.183	6	4	4	0.976	8	3	2	−0.015	9	5	3	0.223	11	10	3	0.059
2	1	1	−1.486	6	5	1	−0.076	8	3	3	−0.117	9	5	4	0.004	11	10	4	0.091
2	2	1	−1.366	6	5	2	−0.085	8	4	1	0.015	9	5	5	−0.122	11	10	5	−0.106
2	2	2	−55.212	6	5	3	0.010	8	4	2	−0.025	9	6	1	−0.007	11	10	6	−0.222
3	1	1	−0.026	6	5	4	−0.026	8	4	3	0.003	9	6	2	−0.128	11	10	7	0.056
3	2	1	0.095	6	5	5	0.051	8	4	4	−0.019	9	6	3	0.100	11	10	8	0.791
3	2	2	−0.003	6	6	1	−3.440	8	5	1	−0.036	9	6	4	0.017	11	10	9	0.322
3	3	1	0.055	6	6	2	−1.126	8	5	2	−0.237	9	6	5	0.020	11	11	1	0.192
3	3	2	0.175	6	6	3	0.075	8	5	3	0.224	9	6	6	−0.163	11	11	2	−1.450
3	3	3	−32.907	6	6	4	−1.673	8	5	4	0.036	9	7	1	0.002	11	11	3	0.333
4	1	1	−1.470	6	6	5	−0.124	8	5	5	−0.036	9	7	2	0.104	11	11	4	0.003
4	2	1	0.077	6	6	6	0.809	8	6	1	−0.106	9	7	3	−0.021	11	11	5	−0.324
4	2	2	−0.905	7	1	1	0.749	8	6	2	0.115	9	7	4	−0.059	11	11	6	−0.055
4	3	1	−0.021	7	2	1	0.112	8	6	3	−0.024	9	7	5	−0.021	11	11	7	−0.215
4	3	2	−0.037	7	2	2	−0.727	8	6	4	−0.004	9	7	6	−0.009	11	11	8	3.157
4	3	3	0.031	7	3	1	−0.022	8	6	5	−0.043	9	7	7	−0.002	11	11	9	2.821
4	4	1	−1.189	7	3	2	−0.081	8	6	6	−0.016	9	8	1	−0.001	12	10	1	−0.444
4	4	2	−1.013	7	3	3	0.043	8	7	1	0.013	9	8	2	−0.038	12	10	2	−0.769
4	4	3	−0.052	7	4	1	1.282	8	7	2	−0.186	9	8	3	−0.190	12	10	3	−0.062
4	4	4	−21.260	7	4	2	−0.693	8	7	3	0.013	9	8	4	0.002	12	10	4	0.239
5	1	1	−0.036	7	4	3	−0.070	8	7	4	−0.081	9	8	5	−0.193	12	10	5	−0.078
5	2	1	−0.016	7	4	4	0.108	8	7	5	0.108	9	8	6	0.015	12	10	6	−0.330
5	2	2	−0.007	7	5	1	−0.022	8	7	6	0.014	9	8	7	0.018	12	10	7	−0.037
5	3	1	0.003	7	5	2	0.145	8	7	7	−0.206	9	8	8	0.421	12	10	8	−0.086
5	3	2	−0.021	7	5	3	0.009	8	8	1	−0.134	9	9	1	−0.075	12	10	9	−0.052
5	3	3	0.055	7	5	4	0.025	8	8	2	−0.283	9	9	2	−0.231	12	11	1	−0.012
5	4	1	−0.026	7	5	5	0.023	8	8	3	−0.211	9	9	3	−0.449	12	11	2	−0.655
5	4	2	0.069	7	6	1	−1.691	8	8	4	−0.087	9	9	4	−0.112	12	11	3	0.126
5	4	3	0.002	7	6	2	0.137	8	8	5	−0.421	9	9	5	−0.210	12	11	4	−0.054
5	4	4	−0.001	7	6	3	−0.018	8	8	6	−0.173	9	9	6	−0.091	12	11	5	−0.035
5	5	1	0.038	7	6	4	−1.705	8	8	7	−0.124	9	9	7	−0.152	12	11	6	−0.042
5	5	2	0.187	7	6	5	−0.018	8	8	8	−0.264	9	9	8	0.416	12	11	7	−0.123
5	5	3	0.063	7	6	6	2.693	9	1	1	0.059	9	9	9	−0.256	12	11	8	0.725
5	5	4	0.050	7	7	1	−1.583	9	2	1	0.013	10	10	1	−4.493	12	11	9	0.394
5	5	5	−33.348	7	7	2	−0.802	9	2	2	−0.128	10	10	2	−2.276	12	12	1	−0.063
6	1	1	−0.569	7	7	3	−0.119	9	3	1	0.037	10	10	3	−0.132	12	12	2	−0.553
6	2	1	−1.055	7	7	4	−2.905	9	3	2	−0.268	10	10	4	−0.591	12	12	3	−0.053
6	2	2	−0.939	7	7	5	0.117	9	3	3	−0.036	10	10	5	−0.168	12	12	4	−0.014
6	3	1	0.029	7	7	6	2.663	9	4	1	0.004	10	10	6	3.111	12	12	5	−0.057
6	3	2	0.165	7	7	7	0.885	9	4	2	0.018	10	10	7	1.850	12	12	6	−0.099
6	3	3	0.006	8	1	1	−0.079	9	4	3	−0.026	10	10	8	−0.130	12	12	7	−0.072
6	4	1	1.321	8	2	1	−0.016	9	4	4	−0.051	10	10	9	−0.076	12	12	8	−0.043
6	4	2	0.154	8	2	2	−0.252	9	5	1	0.001	11	10	1	−0.229	12	12	9	−0.042
6	4	3	−0.028	8	3	1	0.010	9	5	2	−0.019	11	10	2	−1.136				

Table 4 CCSD(T)/AFCVTZ computed values (upper line) of spectroscopic parameters for six isotopomers of $H_2C{=}CClF$ and their comparison with the experimental (lower line) data.[45] For the sextic centrifugal distortion constants, no experimental data are available for these isotopologues

	$CH_2{}^{13}C^{35}ClF$	$^{13}CH_2C^{35}ClF$	$CH_2{}^{13}C^{37}ClF$	$^{13}CH_2C^{37}ClF$	(E)−$CHDC^{35}ClF$	(Z)−$CHDC^{35}ClF$
A_0 / MHz	10 635.063 10 679.359 51	10 316.682 10 358.242 79	10 634.706 10 679.033 48	10 315.754 10 357.368 02	10 369.817 10 409.478 86	9669.620 9710.137 22
B_0 / MHz	5053.180 5090.816 35	4990.536 5028.332 30	4906.649 4943.148 60	4845.719 4882.363 62	4808.470 4844.588 35	5036.998 5075.597 72
C_0 / MHz	3420.988 3442.891 04	3359.031 3380.628 15	3353.134 3374.654 03	3292.676 3313.902 92	3280.949 3301.798 19	3307.467 3328.916 15
Δ_J / kHz	1.380 1.354	1.338 1.313	1.308 1.310	1.268 1.253	1.186 1.188	1.386 1.372
Δ_{JK} / kHz	4.930 4.92	4.757 4.93	4.965 4.54	4.628 5.10	4.216 4.24	4.840 4.944
Δ_K / kHz	5.108 5.10	4.852 4.98	5.139 5.47	5.037 4.89	7.198 7.246	2.151 2.237
δ_J / kHz	0.472 0.462	0.462 0.466	0.441 0.439	0.432 0.424	0.401 0.4042	0.494 0.5022
δ_K / kHz	5.373 5.71	5.085 4.92	5.22 5.85	4.950 4.36	4.592 4.55	5.035 4.874
Φ_J / Hz	0.000 820	0.000 832	0.000 745	0.000 755	0.000 670	0.000 932
Φ_{JK} / Hz	0.0148	0.0133	0.0140	0.0126	0.0104	0.0144
Φ_{KJ} / Hz	−0.0143	−0.0141	−0.0130	−0.0128	−0.0107	−0.0182
Φ_K / Hz	0.0257	0.0270	0.0252	0.0263	0.0345	0.0195
ϕ_J / Hz	0.000 428	0.000 432	0.000 390	0.000 393	0.000 350	0.000 478
ϕ_{JK} / Hz	0.008 93	0.008 25	0.008 44	0.007 80	0.006 65	0.008 76
ϕ_K / Hz	0.0950	0.0861	0.0944	0.0856	0.0838	0.0736
χ_{aa} (Cl) / MHz	−72.1423 −72.9957	−72.4036 −73.2380	−56.8453 −57.5169	−57.0517 −57.7101	−72.490 66 −73.306 26	−72.427 82 −73.255 41
χ_{bb} (Cl) / MHz	38.0177 38.6977	38.2790 38.9472	29.9511 30.4870	30.1575 30.6864	38.366 10 39.010 17	38.303 26 38.938 86
χ_{cc} (Cl) / MHz	34.1246 34.2981	34.1246 34.2909	26.8942 27.0299	26.8942 27.0237	34.124 56 34.296 09	34.124 56 34.316 54
χ_{aa} (D) / MHz					0.2053 0.1882	−0.0421 −0.0374
χ_{bb} (D) / MHz					−0.0942 −0.0844	0.1547 0.1388
χ_{cc} (D) / MHz					−0.1111 −0.1039	−0.1126 −0.1013

which holds for all planar molecules where the c axis is perpendicular to the molecular plane containing the a and b axes. Therefore at least the constants of 5 isotopologues are required to obtain the complete structure given by 9 parameters.

The fit has been carried out using the same weight for all the rotational constants, B_e^i, and employing the recently proposed Molecular Structure Refinement (MSR) program.[65,66] In addition to the availability of different optimization algorithms, this program presents a flexible choise of coordinates (ranging from the common Z-matrix to delocalized internal coordinates of A' symmetry) and an extended error analysis providing t-student distribution confidence intervals besides to the more common standard deviation. Furthermore, it has been equipped with the method of predicate observations[67] to augment the dataset when the number of experimental points is low due to the lack of some isotopic substitutions.

2.3 Complete basis set limit equilibrium geometry

The equilibrium geometry of a molecule can be calculated with accuracy if adequate electron correlation and basis-set convergence are taken into account. The cost-effective coupled cluster theory approach with single and double excitations and including treatments of triple excitations with a perturbative, non-iterative method, CCSD(T), has become the standard for highly accurate theoretical structure computations.[68–71]

These CCSD(T) calculations with sufficiently large basis-sets as the correlated molecular wave functions, are able to deliver an accuracy of about 0.2 to 0.3 pm for bond distances.[72] However, increasing the number of basis functions to reach a near complete basis, the computational cost becomes the main obstacle to perform accurate calculations of molecular parameters.

The problem can be solved using an extrapolation scheme which should speed up the systematic convergence to the complete basis set (CBS) limit.[34] After the development of the family of correlation consistent polarized basis sets with hierarchical structure, cc-pVnZ (n = D(2), T(3), Q(4), 5, ... are the cardinal numbers of the basis sets) by Dunning and coworkers,[49,50] several basis set extrapolation (BSE) methods have been proposed.[51,73–78]

The convergence in the computed structural parameters of the molecular geometry is assumed to have the same functional form of the energy.[79] To be more precise, extrapolation has been carried out on geometric parameters instead of on gradients as would be more justified. Indicating the structural parameter with P, the basis-set extrapolation contributions are

$$P = P_\infty(\mathrm{HF-SCF/A}) + \Delta P_\infty(\mathrm{CCSD(T)/B}) + \Delta P(\mathrm{core/C}) \quad (3)$$

with large basis sets A, smaller basis sets B and a basis set C well suited for the treatment of core correlation. The Hartree-Fock basis set limit is obtained from the consolidated, though empirical, extrapolation formula[80]

$$P_\infty(\mathrm{HF-SCF/A}) = P(\mathrm{HF-SCF/cc-pV}n\mathrm{Z}) + a\exp(-bn) \quad (4)$$

with n the cardinal number of the corresponding members of Dunning's hierarchy basis sets. P_∞ is obtained from three different basis set calculations as

$$P_\infty(\mathrm{HF-SCF/A}) = \frac{P_{n-1}^2 - P_{n-2}P_n}{2P_{n-1} - P_{n-2} - P_n} \quad (5)$$

where $P_n = P(\mathrm{HF-SCF/cc-pV}n\mathrm{Z})$.

The extrapolation due to the correlation to the basis-set limit is obtained from the following two-parameter correction,[79]

$$\Delta P_\infty(\mathrm{CCSD(T)/B}) = \Delta P(\mathrm{CCSD(T)/cc-pV}n\mathrm{Z}) - \frac{c}{n^3} \quad (6)$$

Applying the previous equation with two sequential basis sets, the correction at CBS limit is given by

$$\Delta P_\infty(\mathrm{CCSD(T)/B}) = \frac{(n-1)^3\Delta P_{n-1} - n^3\Delta P_n}{[(n-1)^3 - n^3]} \quad (7)$$

where

$$\Delta P_n = \Delta P(\mathrm{CCSD(T)/cc-pV}n\mathrm{Z}) = P(\mathrm{CCSD(T)/cc-pV}n\mathrm{Z}) - P(\mathrm{HF-SCF/cc-pV}n\mathrm{Z}) \quad (8)$$

Since the correlation contributions have been obtained in the frozen-core approximation in order to minimize the computational cost, the inclusion of Eq. 9 is then necessary. The effect of core-valence electron correlation is obtained taking into account the difference between all-electron and frozen-core calculations:

$$\Delta P(\mathrm{core/C}) = P_{ae}(\mathrm{CCSD(T)/cc-pwCV}n\mathrm{Z}) - P_{fc}(\mathrm{CCSD(T)/cc-pwCV}n\mathrm{Z}) \quad (9)$$

In addition to this composite procedure another extrapolation scheme has been considered based on a mixed exponential and gaussian function[81,82]

$$P_n = P_\infty + d\,e^{-(n-1)} + f\,e^{-(n-1)^2} \quad (10)$$

The structural parameter at CBS limit is calculated from three quantum chemistry calculations and is given by

$$P_\infty = \frac{(e^{4n+1} - e^{2n+3})P_{n+2} + (e^2 - e^{4n})P_{n+1} + (e^{2n+1} - e)P_n}{(e-1)e^{4n} + (e - e^3)e^{2n} + e^2 - e} \quad (11)$$

where

$$P_n = P(\mathrm{CCSD(T)/cc-pV}n\mathrm{Z}) \quad (12)$$

3 Results and discussion

In Table 4, the computed ground-state constants and quartic centrifugal distortion constants are compared with the experimental values given by Leung *et al.*.[45] At present, no experimental data are available for the sextic centrifugal distortion terms of the 6 isotopologues of 1-chloro-1-fluoroethene reported in this Table.

As far as the ground-state rotational constants are concerned, the calculated values are all slightly underestimated with respect to the experimental data. The values of the quartic centrifugal distortion constants are all very close to the experimental ones. Moving to the diagonal elements of the inertial chlorine and deuterium atoms quadrupole coupling tensor χ_{ii}, the calculated values are also in good agreement with the observed values.

The overall agreement between the experimental and theoretical spectroscopic paramenters should be considered more than satisfactory, thus confirming the validity of the chosen level of theory.

The semi-experimental equilibrium structure of 1-chloro-1-fluoroethene has been obtained, as explained in Section 2.2, using the experimental ground-state rotational constants together with the theoretical α-constants deduced from the *ab initio* force field.

The vibrational corrections, $B_e^i - B_0^i$, for all the eight isotopologues of 1-chloro-1-fluoroethene computed at different levels of theory and used in the fits are reported in Table 5. In general, CCSD(T) vibrational corrections are larger than B2PLYP/cc-pVTZ ones that are in turn larger then the B3LYP values.

Table 5 Vibrational corrections, $B_e^i - B_0^i$, in MHz, for the eight isotopologues obtained at different levels of theory and used to fit the molecular structure [a]

	$A_e - A_0$	$B_e - B_0$	$C_e - C_0$
$CH_2C^{35}ClF$	56.605	20.448	19.854
	54.473	20.083	19.429
	53.014	19.576	18.975
$CH_2C^{37}ClF$	54.519	19.931	19.150
	54.530	19.438	18.932
	53.104	18.769	18.407
$CH_2{}^{13}C^{35}ClF$	53.482	20.009	19.307
	53.481	19.539	19.055
	52.031	19.052	18.611
$^{13}CH_2C^{35}ClF$	51.189	20.760	19.337
	51.410	20.168	19.058
	50.057	19.673	18.622
$CH_2{}^{13}C^{37}ClF$	53.553	19.295	18.781
	53.537	18.904	18.561
	52.278	18.305	18.087
$^{13}CH_2C^{37}ClF$	51.286	20.014	18.818
	51.481	19.503	18.570
	50.175	18.824	18.055
(E)$-CHDC^{35}ClF$	47.019	20.693	18.579
	47.400	20.032	18.283
	46.014	19.499	17.834
(Z)$-CHDC^{35}ClF$	47.704	20.333	18.751
	47.726	19.997	18.577
	46.689	19.390	18.126

[a] Each set of lines for each isotopologue refers, from top to bottom, to the CCSD(T)/AFCVTZ, B2PLYP/cc-pVTZ and B3LYP/SNSD level of theory, respectively.

The semi-experimental equilibrium geometry has been obtained from a non-linear least square fitting procedure based on Eq. 2 since the equilibrium rotational constants B_e^i depend on the moments of inertia at the equilibrium geometry which, in the Born-Oppenheimer approximation, is the same for all the isotopic modifications of 1-chloro-1-fluoroethene. The differences in B_e^i are therefore due to differences in isotope masses. In particular, the semi-experimental equilibrium structure of 1-chloro-1-fluoroethene has been obtained according to three different fits in which CCSD(T), B2PLYP, B3LYP vibrational corrections have been employed and the results are collected in Table 6 labeled as $r_e^{SE}(CC)$, $r_e^{SE}(B2)$, $r_e^{SE}(B3)$, respectively. As it can be seen the three fits provide the same equilibrium geometry of $ClFC{=}CH_2$ with differences in bond lengths and angles well within 0.002 Å and 0.2 degrees respectively, thus supporting the consistency of the vibrational corrections computed by using the cost-effective B2PLYP/cc-pVTZ and B3LYP/SNSD model chemistries.

Table 6 Semi-experimental structure of 1-chloro-1-fluoroethene obtained by using vibrational corrections computed at the coupled cluster and DFT levels (bond lengths in Å, bond angles in degrees)

	$r_e^{SE}(CC)^{a,b}$	$r_e^{SE}\ (B2)^{a,c}$	$r_e^{SE}\ (B3)^{a,d}$
C_2-F_1	1.3287(52)	1.3294(8)	1.3282(1)
	0.012	0.0018	0.0042
$C_2=C_3$	1.3233(37)	1.3220(6)	1.3224(1)
	0.0089	0.0013	0.0030
C_3-H_4	1.0780(13)	1.0780(2)	1.0777(4)
	0.0030	0.00045	0.0010
C_2-Cl_5	1.7081(31)	1.7089(5)	1.7099(1)
	0.0073	0.0011	0.0025
C_3-H_6	1.0750(16)	1.0765(2)	1.0762(5)
	0.0037	0.00055	0.0013
$\angle C_3C_2F_1$	125.44(30)	122.48(4)	122.56(10)
	0.70	0.10	0.24
$\angle C_3C_2Cl_5$	125.52(32)	125.61(5)	125.54(1)
	0.75	0.11	0.26
$\angle C_2C_3H_6$	120.02(23)	119.85(3)	119.90(8)
	0.53	0.08	0.18
$\angle C_2C_3H_4$	119.30(20)	119.33(3)	119.30(7)
	0.48	0.08	0.16

[a] Figures in parentheses represents one time the standard deviation. The numbers below the values of the structural parameters are 95% confidence intervals from t-Student distribution.

[b] Vibrational corrections at CCSD(T)/AFCVTZ.

[c] Vibrational corrections at B2PLYP/cc-pVTZ level.

[d] Vibrational corrections at B3LYP/SNSD level.

As far as the complete basis set limit equilibrium geometry is concerned, the contributions to the structural parameters of Eq. 3 have been computed as described below. The Hartree-Fock basis-set limit and the unknown parameters a and b of Eq. 4 have been determined from three calculations employing sequential basis sets. Choosing $n = 6$, P_∞ can be easily obtained from Eq. 5 employing the results of Hartree-Fock calculations with cc-pVQZ, cc-pV5Z, and cc-pV6Z basis sets. The corrections due to the correlation have been calculated from Eq. 7 and $n = 5$. Therefore, at CCSD(T) level of theory the quantum chemical computations have been carried out with cc-pVQZ and cc-pV5Z basis sets. Although the TZ and QZ basis sets could be sufficient for this contribution because they require less computational time, the larger basis sets have been used here since they are also necessary for the other extrapolation method as explained below. For the last contribution, the inner-shell correlations have been computed with the weighted core-valence cc-pwCVQZ set[52] in Eq. 9.

For the extrapolation scheme described in Eq. 10, three calculations are necessary in order to get the structural parameter at CBS limit with Eq. 11. Using $n = 3$, the calculations have been

Table 7 Equilibrium geometries of 1-chloro-1-fluoroethene as computed at different levels of theory employing different basis sets (see text). Distances in Å and angles in degrees

	HF-SCF/cc-pV*n*Z			CCSD(T)/cc-pV*n*Z			CCSD(T)/cc-pwCVQZ	
	Q	5	6	T	Q	5	fc	ae
C_2-F_1	1.3051	1.3053	1.3053	1.3304	1.3294	1.3299	1.3295	1.3275
$C_2=C_3$	1.3034	1.3035	1.3035	1.3286	1.3255	1.3251	1.3253	1.3224
C_3-H_4	1.0709	1.0708	1.0707	1.0800	1.0793	1.0792	1.0793	1.0778
C_2-Cl_5	1.7146	1.7123	1.7121	1.7245	1.7183	1.7140	1.7145	1.7108
C_3-H_6	1.0679	1.0678	1.0678	1.0775	1.0769	1.0768	1.0769	1.0755
$\angle C_3C_2F_1$	123.01	122.93	122.93	122.70	122.67	122.54	122.59	122.59
$\angle C_3C_2Cl_5$	125.39	125.44	125.44	125.24	125.37	125.51	125.40	125.40
$\angle C_2C_3H_6$	120.53	120.52	120.52	120.17	120.03	119.98	120.02	120.06
$\angle C_2C_3H_4$	119.52	119.55	119.56	119.30	119.33	119.33	119.34	119.36

carried out employing cc-pVTZ, cc-pVQZ, and cc-pV5Z basis sets at CCSD(T) level of theory.

The molecular geometries of 1-chloro-1-fluoroethene obtained from these calculations are reported in Table 7.

Below the line reporting the theoretical method, the cardinal number of Dunning's hierarchical basis-set sequences is also indicated. To be more precise, three values (Q, 5, and 6) are for HF-SCF calculations, and other three values (T, Q, and 5) for CCSD(T) method. The last two columns are relative to the core-valence contribution and report the frozen core (fc) calculation as well as the computation correlating all the electrons (ae).

As far as the Hartree-Fock Self-Consistent-Field computations are concerned, it is confirmed – as often assumed – that the basis set limit is reached with the HF-SCF/cc-pV6Z level of theory. Concerning the coupled cluster calculations, from the data shown in Table 7, we can see a progressive smooth increase or decrease, with the exception of the C−F bond length (probably due to the lack of the diffuse functions which are present in the augmented basis set), in the value of the structural parameter when we change from $n = 3$ (T) to $n = 5$.

Table 8 Complete basis set equilibrium molecular structures of 1-chloro-1-fluoroethene applying Eq. 3 (CBS-I) and Eq. 11 (CBS-II) (bond lengths in Å, bond angles in degrees). Δ_{CC} is the coupled cluster correlation contribute from Eq. 7 and Δ_{CV}, from Eq. 9, is the core-valence correction

	Δ_{CC}	Δ_{CV}	CBS−I	CBS−II
C_2-F_1	0.0250	−0.0020	1.3283	1.3282
$C_2=C_3$	0.0210	−0.0029	1.3216	1.3219
C_3-H_4	0.0083	−0.0014	1.0777	1.0776
C_2-Cl_5	−0.0003	−0.0037	1.7081	1.7078
C_3-H_6	0.0091	−0.0014	1.0754	1.0754
$\angle C_3C_2F_1$	−0.44	0.00	122.48	122.47
$\angle C_3C_2Cl_5$	0.16	−0.01	125.59	125.58
$\angle C_2C_3H_6$	−0.59	0.03	119.96	119.98
$\angle C_2C_3H_4$	−0.25	0.01	119.32	119.35

Applying Eqs. 5, 7, and 9 with the data reported in Table 7, all the contributions necessary to employ Eq. 3 could be determined. For the sake of completeness, in the first and in the second column of Table 8 are reported the coupled cluster contribute from Eq. 7 and the core-valence correlation of Eq. 9, respectively. The complete basis set structure obtained is reported in Table 8 labeled as CBS-I. Using the mixed exponential and gaussian function resulting in Eq. 11 the molecular structure, indicated in Table 8 as CBS-II, is obtained. The two molecular geometries, CBS-I and CBS-II, are almost equivalent, with a maximum difference in the bonding distance 0.003 Å while the bond angles differ at most 0.03°. It should however be pointed out that CBS-II requires 3 calculations against the 7 required by CBS-I. On the opposite, DFT geometries, reported in Table 9, show significant differences with respect to the semi-experimental structure. At B2PLYP/cc-pVTZ level of theory, bond lengths and angles are reproduced quite well with a mean absolute deviation (MAD) of 0.005 Å and 0.2°, however with a maximum deviation of 0.02 Å for the C−Cl bond length. As to the B3LYP/SNSD level of theory, the errors are larger and up to 0.03 Å for the C−Cl bond length and 0.5° for the CCCl bond angle. As noted, B3LYP/SNSD and B2PLYP/cc- pVTZ predictions of 1-chloro-1-fluoroethene geometrical parameters suffer from large inaccuracy with respect to the semi-experimental parameters. A possible strategy to improve DFT results is given by the LRA. This is based on the observation that DFT errors are systematic and follow a linear trend and hence it is possible to obtain a linear transformation for back-correcting structural parameters:

$$r_e^{LRA} = r_e^{DFT} + \Delta r \qquad \text{with} \qquad \Delta r = A r_e^{DFT} + B \tag{13}$$

where A and B are, respectively, (1-slope) and the intercept obtained by performing a linear regression of a semi-experimental structural parameter as a function of the corresponding DFT value. For C−H, C=C, C−F, and C−Cl bond lengths, the LRA has been applied by adopting the regression parameters A and B determined in previous works by Barone and co-workers[38,66] and derived from a set of 100, 45, 6 and 5 items, respectively. The interested reader is referred to the cited literature and to the SNS structural database[39] for further details on the molecules used to

Table 9 Equilibrium geometries of 1-chloro-1-fluoroethene computed at B2PLYP/cc-pVTZ and B3LYP/SNSD levels. Distances in Å and angles in degrees

	B2PLYP	B2PLYP+LRA[a]	B3LYP	B3LYP+LRA[b]
C_2-F_1	1.3306	1.3281	1.3372	1.3278
$C_2=C_3$	1.3206	1.3218	1.3247	1.3220
C_3-H_4	1.0776	1.0778	1.0838	1.0780
C_2-Cl_5	1.7236	1.7115	1.7369	1.7094
C_3-H_6	1.0785	1.0786	1.0811	1.0755
$\angle C_3C_2F_1$	122.83	122.33	122.80	122.43
$\angle C_3C_2Cl_5$	125.39	125.39 [c]	125.70	125.39 [c]
$\angle C_2C_3H_6$	120.38	120.38 [c]	120.49	120.38 [c]
$\angle C_2C_3H_4$	119.32	119.32 [c]	119.5	119.32 [c]

[a] B2PLYP/cc-pVTZ equilibrium geometry corrected through the LRA approach (see text). [b] B3LYP/SNSD equilibrium geometry corrected through the LRA approach (see text). [c] Uncorrected value.

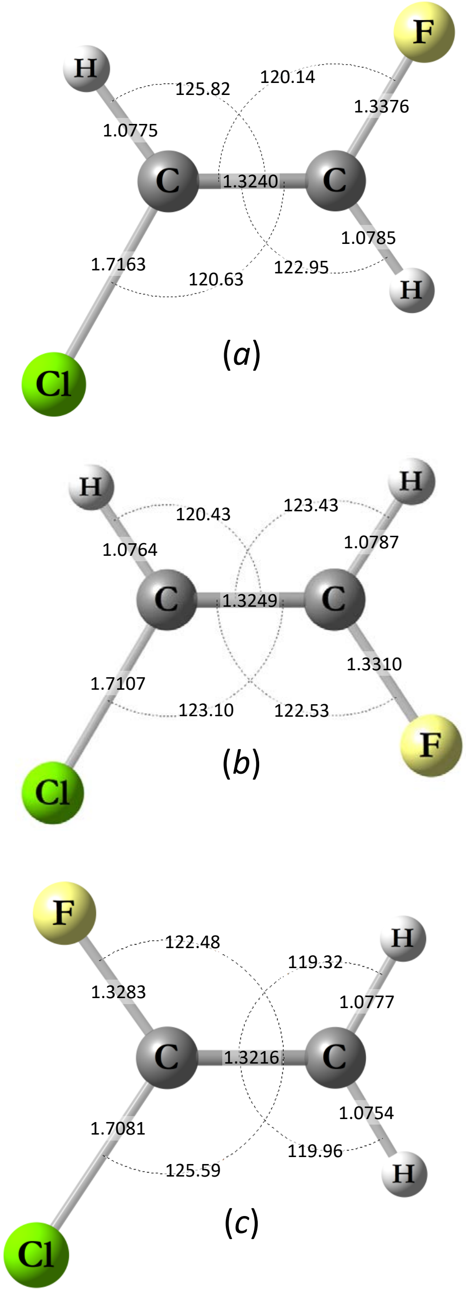

Fig. 2 Comparison of the best theoretical estimate for the equilibrium structure of (*a*) *trans*-1-chloro-2-fluoroethene [83], (*b*) *cis*-1-chloro-2-fluoroethene [83], (*c*) 1-chloro-1-fluoroethene. Distances in Å and angles in deg.

set up both the LRA and the TMA.[37,38,66] In the present work, it has been possible to obtain a new LRA correction for the CCF bond angle ($A = -0.13136$, $B = 15.63107$ for B2PLYP/cc-pVTZ; $A = -0.12032$, $B = 14.40384$ for B3LYP/SNSD), by using in addition to the CCF parameter of 1-chloro-1-fluoroethene those of vinylfluoride, *cis*-CHFCHCl, 2-fluoropyridine and 3-fluoropyridine already present in the SMART database of molecular structures.[39] Table 9 reports the results of this procedure.

Even if the number of items employed to obtain the A and B parameters for the CCF bond angle is limited, the linear regressions present an $R^2 = 0.995$. Moreover, it can be observed how the LRA improves the description of this angle that at B2PLYP and B3LYP levels is predicted with an error of 0.4° that reduces to $-0.1°$ and 0.01° when the LRA is applied to the B2PLYP/cc-pVTZ and B3LYP/SNSD values, respectively. Very notably, when the LRA correction is applied to the C-Cl bond length, that was badly predicted at both B2PLYP and B3LYP levels, the error is reduced by about one order of magnitude. LRA corrected bond lengths present a MAD around 0.001 Å thus showing the effectiveness of this scheme, whose accuracy competes with that of highly-correlated wavefunction methods however with a significantly lower computational cost.

Taking as a reference the CBS-I theoretical equilibrium structure reported in the third column of Table 8, chemically relevant structural comparison with the best theoretical equilibrium structures of *cis*-1-chloro-2-fluoroethene and *trans*-1-chloro-2-fluoroethene reported by Puzzarini *et al.*,[83] can be discussed.

Figure 2 features these data showing the molecular geometry of the three isomers of chlorofluoroethene. Although not all parameters can be compared appropriately some considerations can still be carried out. At first we note that the CH_2 group is very close to the trigonal geometry, being the angles almost 120°. The C−H distances remain rather unchanged upon isomerization. The largest effects are observed for the C−Cl and C−F distances. The C−Cl distance in the *gem* compound is shortened by 0.0082 Å with respect to the *trans* and by 0.0026 Å compared to the *cis* form. Similar behavior is observed for the C−F distance which is shortened by 0.0093 Å and 0.0027 Å, respectively, when compared to the *trans*- and *cis*-isomer. The changes in the CCF and CCCl bond angles in the *cis*- and *trans*-isomers were explained invoking the steric effects, as the fluorine and chlorine atoms move away from each other. In the *gem* isomer the decrease of the FCCl angle to 111.93° of course cannot be explained by steric hindrance and should therefore be due to the electronic arrangement of the molecular orbitals. It should also be mentioned that in 1,1-dichloroethene and 1,1-difluoroethene the angles ClCCl and FCF are, respectively, 117.8° and 115.5°, as determined in the r_s molecular structure.[84] Finally, it must be considered the C=C bond length; we note that this bond distance is shortened further than the *cis* and *trans* values, confirming the well-known effect induced by substitution of one or more hydrogens by halogens.[85]

4 Conclusions

One of the present challenges of quantum chemistry is the accurate prediction of equilibrium geometries for systems of increasing size, this being a fundamental prerequisite for the reliable modeling of spectroscopic properties. In this context, the knowledge of the semi-experimental equilibrium structure of small molecules serves as cornerstone in building up new cost-effective methodologies or theoretical approaches. In the present work, the accurate equilibrium geometry of 1-chloro-1-fluoroethene has been first obtained by exploiting the semi-experimental approach and using vibrational corrections evaluated at three different levels of theory, namely CCSD(T), B2PLYP and B3LYP. These have led to the same geometrical parameters, thus confirming the reliability of vibrational contributions evaluated at DFT level. The obtained semi-experimental equilibrium structure has then been compared with those obtained by exploiting two different composite schemes based on the CCSD(T) theory and accounting for extrapolation to the CBS and inclusion of core-valence correlation. The two approaches have led to the same equilibrium geometry whose agreement with the semi-experimental structure is within 0.002 Å and 0.1° for bond lengths and angles, respectively. Conversely, geometries optimized at B2PLYP and B3LYP levels have shown significant errors. The structural parameters have been improved by applying the LRA, thus providing DFT-based structures with an accuracy rivalling that of highly correlated wavefunction methods. Hence, the LRA appears as a cost-effective strategy for determining accurate equilibrium geometries through DFT thus disclosing the route toward medium sized molecular systems. However, the parametrization of the linear transformations behind the LRA for different geometrical parameters requires the careful investigation of the semi-experimental equilibrium geometries for a variety of molecules thus also improving the available database of accurate equilibrium structures.

Conflicts of interest

There are no conflicts to declare.

Acknowledgements

This work has been supported by MIUR "PRIN 2015" funds (Grant Number 2015F59J3R), by Scuola Normale Superiore (GR16_B_TASINATO) and University Ca' Foscari Venezia (ADiR funds). The SMART@SNS Laboratory (http://smart.sns.it) is acknowledged for providing high-performance computer facilities. GC thanks SNS for her research fellowship.

References

1 T.-D.-H. Vo, C. Lin, C.-E. Weng, C.-S. Yuan, C.-W. Lee, C.-H. Hung, X.-T. Bui, K.-C. Lo and J.-X. Lin, *J. Environ. Manage.*, 2018, **217**, 327 – 336.

2 C. Dai, Y. Zhou, H. Peng, S. Huang, P. Qin, J. Zhang, Y. Yang, L. Luo and X. Zhang, *J. Ind. Eng. Chem.*, 2018, **62**, 106 – 119.

3 Q. Zhang, Y. Chen, S. Tong, M. Ge, J. Shenolikar, M. S. Johnson, Y. Wang, N. T. Tsona, A. Mellouki and L. Du, *Atmos. Environ.*, 2017, **170**, 12 – 21.

4 B. Huang, C. Lei, C. Wei and G. Zeng, *Environ. Int.*, 2014, **71**, 118 – 138.

5 D. McNaughton, E. G. Robertson, C. D. Thompson, T. Chimdi, M. K. Bane and D. Appadoo, *Anal. Chem.*, 2010, **82**, 7958–7964.

6 C. J. Evans, A. Sinik, C. Medcraft, D. McNaughton, D. Appadoo and E. G. Robertson, *J. Phys. Chem. A*, 2014, **118**, 2480–2487.

7 A. Wong, C. D. Thompson, D. R. Appadoo, R. Plathe, P. Roy, L. Manceron, J. Barros and D. McNaughton, *Mol. Phys.*, 2013, **111**, 2198–2203.

8 G. Cazzoli, L. Cludi, C. Puzzarini, P. Stoppa, A. Pietropolli Charmet, N. Tasinato, A. Baldacci, A. Baldan, S. Giorgianni, R. W. Larsen, S. Stopkowicz and J. Gauss, *J. Phys. Chem. A*, 2011, **115**, 453–459.

9 A. Pietropolli Charmet, N. Tasinato, P. Stoppa, A. Baldacci and S. Giorgianni, *Mol. Phys.*, 2008, **106**, 1171–1179.

10 A. Baldacci, P. Stoppa, A. Pietropolli Charmet, S. Giorgianni, G. Cazzoli, C. Puzzarini and R. W. Larsen, *J. Phys. Chem. A*, 2007, **111**, 7090–7097.

11 I. Sadiek, Q. Shi, D. W. R. Wallace and G. Friedrichs, *Anal. Chem.*, 2017, **89**, 8445–8452.

12 N. Tasinato, A. Pietropolli Charmet, P. Stoppa and S. Giorgianni, *Mol. Phys.*, 2010, **108**, 677–685.

13 N. Tasinato, A. Turchetto, C. Puzzarini, P. Stoppa, A. Pietropolli Charmet and S. Giorgianni, *Mol. Phys.*, 2014, **112**, 2384–2396.

14 E. G. Robertson, C. Medcraft, D. McNaughton and D. Appadoo, *J. Phys. Chem. A*, 2014, **118**, 10944–10954.

15 W. Fuß, E. G. Robertson, C. Medcraft and D. R. T. Appadoo, *J. Phys. Chem. A*, 2014, **118**, 5391–5399.

16 N. Tasinato, P. Stoppa, A. Pietropolli Charmet, S. Giorgianni and A. Gambi, *J. Quant. Spectrosc. Radiat. Transf.* , 2012, **113**, 1240–1249.

17 N. Tasinato, P. Stoppa, A. Pietropolli Charmet, S. Giorgianni, G. Buffa and A. Gambi, *ChemPhysChem*, 2011, **12**, 356–363.

18 M. Hochlaf, *Phys. Chem. Chem. Phys.*, 2017, **19**, 21236–21261.

19 M. Piccardo, J. Bloino and V. Barone, *Int. J. Quantum Chem.*, 2015, **115**, 948–982.

20 A. G. Császár, C. Fábri, T. Szidarovszky, E. Mátyus, T. Furtenbacher and G. Czáko, *Phys. Chem. Chem. Phys.*, 2012, **14**, 1085–1106.

21 S. Albert, E. Bekhtereva, I. Bolotova, Z. Chen, C. Fábri, H. Hollenstein, M. Quack and O. Ulenikov, *Phys. Chem. Chem. Phys.*, 2017, **19**, 26527–26534.

22 A. Pietropolli Charmet, P. Stoppa, S. Giorgianni, J. Bloino, N. Tasinato, I. Carnimeo, M. Biczysko and C. Puzzarini, *J. Phys. Chem. A*, 2017, **121**, 3305–3317.

23 S. V. Krasnoshchekov, N. C. Craig and N. F. Stepanov, *J. Phys. Chem. A*, 2013, **117**, 3041–3056.

24 A. Pietropolli Charmet, P. Stoppa, N. Tasinato, S. Giorgianni, V. Barone, M. Biczysko, J. Bloino, C. Cappelli, I. Carnimeo and C. Puzzarini, *J. Chem. Phys.*, 2013, **139**, 164302.

25 N. Tasinato, A. Pietropolli Charmet, P. Stoppa, S. Giorgianni and A. Gambi, *Chem. Phys.*, 2012, **397**, 55 – 64.

26 A. Pietropolli Charmet, N. Tasinato, P. Stoppa, S. Giorgianni and A. Gambi, *Mol. Phys.*, 2011, **109**, 2163–2172.

27 D. C. McKean, M. M. Law, P. Groner, A. R. Conrad, M. J. Tubergen, D. Feller, M. C. Moore and N. C. Craig, *J. Phys. Chem. A*, 2010, **114**, 9309–9318.

28 A. Pietropolli Charmet, P. Stoppa, N. Tasinato, A. Baldan, S. Giorgianni and A. Gambi, *J. Chem. Phys.*, 2010, **133**, 044310.

29 N. Tasinato, G. Regini, P. Stoppa, A. Pietropolli Charmet and A. Gambi, *J. Chem. Phys.*, 2012, **136**, 214302.

30 C. Puzzarini and V. Barone, *Acc. Chem. Res.*, 2018, **51**, 548–

556.

31 C. Puzzarini, *Int. J. Quantum Chem.*, 2016, **116**, 1513–1519.

32 W. Gordy and R. L. Cook, *Microwave molecular spectra*, Wiley, New York, 1984, 3rd Edition.

33 M. Heckert, M. Kállay and J. Gauss, *Mol. Phys.*, 2005, **103**, 2109–2115.

34 M. Heckert, M. Kállay, D. P. Tew, W. Klopper and J. Gauss, *J. Chem. Phys.*, 2006, **125**, 044108.

35 V. Barone, M. Biczysko, J. Bloino and C. Puzzarini, *Phys. Chem. Chem. Phys.*, 2013, **15**, 10094–10111.

36 P. Pulay, W. Meyer and J. Boggs, *J. Chem. Phys.*, 1978, **68**, 5077–5085.

37 M. Piccardo, E. Penocchio, C. Puzzarini, M. Biczysko and V. Barone, *J. Phys. Chem. A*, 2015, **119**, 2058–2082.

38 E. Penocchio, M. Piccardo and V. Barone, *J. Chem. Theory Comput.*, 2015, **11**, 4689–4707.

39 http://smart.sns.it/, accessed 23/06/2018.

40 E. Brémond, M. Savarese, N. Su, A. Pérez-Jiménez, X. Xu, J. Sancho-García and C. Adamo, *J. Chem. Theory Comput.*, 2016, **12**, 459–465.

41 R. Peverati and D. Truhlar, *Philos. Trans. R. Soc. London, Ser. A*, 2014, **372**, 20120476.

42 S. Grimme and M. Steinmetz, *Phys. Chem. Chem. Phys.*, 2013, **15**, 16031–16042.

43 R. G. Stone and W. H. Flygare, *J. Mol. Spectrosc.*, 1969, **32**, 233–241.

44 J. L. Alonso, A. G. Lesarri, L. A. Leal and J. López, *J. Mol. Spectrosc.*, 1993, **162**, 4–19.

45 H. O. Leung, M. D. Marshall, A. L. Vasta and N. C. Craig, *J. Mol. Spectrosc.*, 2009, **253**, 116–121.

46 K. Raghavachari, G. W. Trucks, J. A. Pople and M. Head-Gordon, *Chem. Phys. Lett.*, 1989, **157**, 479–483.

47 CFOUR, Coupled-Cluster techniques for Computational Chemistry, a quantum-chemical program package written by J.F. Stanton, J. Gauss, L. Cheng, M.E. Harding, D.A. Matthews, P.G. Szalay *et al.*, and the integral packages MOLECULE (J. Almlöf and P.R. Taylor), PROPS (P.R. Taylor), ABACUS (T. Helgaker, H.J. Aa. Jensen, P. Jørgensen, and J. Olsen), and ECP routines by A. V. Mitin and C. van Wüllen. For the current version, see http://www.cfour.de.

48 A. Pietropolli Charmet, P. Stoppa, N. Tasinato, S. Giorgianni and A. Gambi, *J. Phys. Chem. A*, 2016, **120**, 8369–8386.

49 T. H. Dunning Jr, *J. Chem. Phys.*, 1989, **90**, 1007–1023.

50 D. E. Woon and T. H. Dunning Jr, *J. Chem. Phys.*, 1995, **103**, 4572–4585.

51 D. E. Woon and T. H. Dunning Jr, *J. Chem. Phys.*, 1993, **99**, 1914–1928.

52 K. A. Peterson and T. H. Dunning Jr, *J. Chem. Phys.*, 2002, **117**, 10548–10560.

53 J. Gauss and J. F. Stanton, *Chem. Phys. Lett.*, 1997, **276**, 70–77.

54 W. Schneider and W. Thiel, *Chem. Phys. Lett.*, 1989, **157**, 367–373.

55 J. F. Stanton, C. L. Lopreore and J. Gauss, *J. Chem. Phys.*, 1998, **108**, 7190–7196.

56 P. Pyykkö, *Z. Naturforsch., Part A.*, 1992, **47**, 189–196.

57 C. Lee, W. Yang and R. Parr, *Phys. Rev. B*, 1988, **37**, 785–789.

58 A. Becke, *J. Chem. Phys.*, 1993, **98**, 5648–5652.

59 I. Carnimeo, C. Puzzarini, N. Tasinato, P. Stoppa, A. Pietropolli Charmet, M. Biczysko, C. Cappelli and V. Barone, *J. Chem. Phys.*, 2013, **139**, 074310.

60 S. Grimme, *J. Chem. Phys.*, 2006, **124**, 034108.

61 M. J. Frisch, G. W. Trucks, H. B. Schlegel, G. E. Scuseria, M. A. Robb, J. R. Cheeseman, G. Scalmani, V. Barone, G. A. Petersson, H. Nakatsuji, X. Li, M. Caricato, A. V. Marenich, J. Bloino, B. G. Janesko, R. Gomperts, B. Mennucci, H. P. Hratchian, J. V. Ortiz, A. F. Izmaylov, J. L. Sonnenberg, D. Williams-Young, F. Ding, F. Lipparini, F. Egidi, J. Goings, B. Peng, A. Petrone, T. Henderson, D. Ranasinghe, V. G. Zakrzewski, J. Gao, N. Rega, G. Zheng, W. Liang, M. Hada, M. Ehara, K. Toyota, R. Fukuda, J. Hasegawa, M. Ishida, T. Nakajima, Y. Honda, O. Kitao, H. Nakai, T. Vreven, K. Throssell, J. A. Montgomery, Jr., J. E. Peralta, F. Ogliaro, M. J. Bearpark, J. J. Heyd, E. N. Brothers, K. N. Kudin, V. N. Staroverov, T. A. Keith, R. Kobayashi, J. Normand, K. Raghavachari, A. P. Rendell, J. C. Burant, S. S. Iyengar, J. Tomasi, M. Cossi, J. M. Millam, M. Klene, C. Adamo, R. Cammi, J. W. Ochterski, R. L. Martin, K. Morokuma, O. Farkas, J. B. Foresman and D. J. Fox, *Gaussian 16 Revision B.01*, 2016, Gaussian Inc. Wallingford CT.

62 J. Bloino, M. Biczysko and V. Barone, *J. Chem. Theory Comput.*, 2012, **8**, 1015–1036.

63 I. M. Mills, in *Molecular Spectroscopy: Modern Research*, ed. K. N. Rao and C. W. Mathews, Academic Press, New York, 1972, pp. 115 – 140.

64 D. Papoušek and M. R. Aliev, *Molecular Vibrational-Rotational Spectra*, Academia, Prague, 1982.

65 M. Mendolicchio, E. Penocchio, D. Licari, N. Tasinato and V. Barone, *J. Chem. Theory Comput.*, 2017, **13**, 3060–3075.

66 E. Penocchio, M. Mendolicchio, N. Tasinato and V. Barone, *Can. J. Chem.*, 2016, **94**, 1065–1076.

67 L. Bartell, D. Romanesko, T. Wong, G. Sims and L. Sutton, in *Molecular Structure by Diffraction Methods: Volume 3*, ed. G. A. Sim and L. E. Sutton, The Chemical Society, Specialist Periodical Report, 1975, pp. 72 – 80.

68 C. Puzzarini, M. Biczysko, J. Bloino and V. Barone, *Astrophys J.*, 2014, **785**, 107.

69 C. Puzzarini, J. Stanton and J. Gauss, *Int. Rev. Phys. Chem.*, 2010, **29**, 273–367.

70 P. Tentscher and J. Arey, *J. Chem. Theory Comput.*, 2012, **8**, 2165–2179.

71 R. Ramabhadran and K. Raghavachari, *J. Chem. Theory Comput.*, 2013, **9**, 3986–3994.

72 K. L. Bak, J. Gauss, P. Jørgensen, J. Olsen, T. Helgaker and J. F. Stanton, *J. Chem. Phys.*, 2001, **114**, 6548–6556.

73 D. Feller, *J. Chem. Phys.*, 1992, **96**, 6104–6114.

74 D. Feller, *J. Chem. Phys.*, 1993, **98**, 7059–7071.

75 J. M. L. Martin and P. R. Taylor, *Chem. Phys. Lett.*, 1996, **248**,

336–344.
76 K. A. Peterson and T. H. Dunning Jr, *J. Mol. Struct. (THEOCHEM)*, 1997, **400**, 93–117.
77 B. J. Persson, P. R. Taylor and J. M. L. Martin, *J. Phys. Chem. A*, 1998, **102**, 2483–2492.
78 C. Puzzarini, *J. Phys. Chem. A*, 2009, **113**, 14530–14535.
79 T. Helgaker, W. Klopper, H. Koch and J. Noga, *J. Chem. Phys.*, 1997, **106**, 9639–9646.
80 A. Halkier, T. Helgaker, P. Jørgensen, W. Klopper and J. Olsen, *Chem. Phys. Lett.*, 1999, **302**, 437–446.
81 K. A. Peterson, D. E. Woon and T. H. Dunning Jr, *J. Chem. Phys.*, 1994, **100**, 7410–7415.
82 D. Feller and K. A. Peterson, *J. Chem. Phys.*, 1999, **110**, 8384–8396.
83 C. Puzzarini, G. Cazzoli, A. Gambi and J. Gauss, *J. Chem. Phys.*, 2006, **125**, 054307.
84 H. Takeo, M. Sugie and C. Matsumura, *J. Mol. Struct.*, 1988, **190**, 205 – 214.
85 J. Demaison, H. Møllendal, A. Perrin, J. Orphal, F. K. Tchana, H. Rudolph and F. Willaert, *J. Mol. Spectrosc.*, 2005, **232**, 174 – 185.